

Jet color chemistry and anomalous baryon production in AA -collisions

P. Aurenche^a and B.G. Zakharov^b

^a *LAPTH, Université de Savoie, CNRS,
BP 110, F-74941, Annecy-le-Vieux Cedex, France*

^b *L.D. Landau Institute for Theoretical Physics, GSP-1, 117940,
Kosygina Str. 2, 117334 Moscow, Russia*

Abstract

We study anomalous high- p_T baryon production in AA -collisions due to formation of the two parton collinear gq system in the anti-sextet color state for quark jets and gg system in the decuplet/anti-decuplet color states for gluon jets. Fragmentation of these states, which are absent for NN -collisions, after escaping from the quark-gluon plasma leads to baryon production. Our qualitative estimates show that this mechanism can be potentially important at RHIC and LHC energies.

1 Introduction

One of the intriguing results from the RHIC program (for a review, see [1]) is the significant enhancement of the baryon/meson ratios in AA -collisions at $1.5 \lesssim p_T \lesssim 5$ GeV [2, 3, 4], the so-called “baryon anomaly”. The underlying mechanisms of this effect remain not well understood. It has been suggested [5, 6] that the physical reason for the baryon anomaly may lie in the enhancement of the string junction (SJ) loops in the quark-gluon plasma (QGP) produced in AA -collisions. The notion of SJ was introduced by Rossi and Veneziano [7, 8] in the generalization of the topological expansion scheme [9] to the processes with baryons. In the Rossi-Veneziano approach [7, 8] the baryons have a Y -shaped string configuration, and the string junction trajectory is the intersection of three planar sheets. The SJ concept arises naturally from the gauge-invariant expression of the operator with baryon quantum numbers

$$B_{\alpha\beta\gamma} = \epsilon^{i_1 i_2 i_3} \left[P \exp \int_{p(x, x_1)} A_\mu dx^\mu q_\alpha(x_1) \right]_{i_1} \left[P \exp \int_{p(x, x_2)} A_\mu dx^\mu q_\beta(x_2) \right]_{i_2} \\ \times \left[P \exp \int_{p(x, x_3)} A_\mu dx^\mu q_\gamma(x_3) \right]_{i_3}. \quad (1)$$

The Y -configuration for baryons is now supported by the lattice simulation [10, 11]. But there have not so far been proposed dynamical computational methods for the SJ effects neither in high energy hadron collisions nor in hadronization of the expanding QGP. For

this reason the SJ model [5] remains highly speculative, and the connection of the SJ loops to the baryon anomaly needs elucidation.

In the model of SJ loops [5] the baryon/meson enhancement in AA -collisions is not a fragmentation effect, but is a specific soft effect of plasma hadronization extending to moderate p_T . Another soft mechanism, which can potentially contribute to the anomalous baryon production in AA -collisions, is the quark recombination/coalescence [12, 13, 14] (for a review, see [15]). Since baryons produced via a quark clustering receive larger transverse momentum than mesons it can lead to an enhancement of the baryon/meson ratios. The recombination models have had considerable success in explaining the dependence of the hadron spectra on the number of constituent quarks. Unfortunately, the recombination picture does not have a firm first-principle theoretical justification at present. In particular, the possibility of neglecting parton interactions in the hadronization process, which is the basic assumption of the recombination model, remains an open question. The mechanism of the quark dominance in the clustering process remains unclear as well.

In the present paper we discuss a mechanism for the anomalous baryon production, which, contrary to the SJ loops and recombination mechanisms, is related to the color dynamics of fast partons, and persists at high p_T . It has been proposed in [16], several years before the experimental observation of the baryon anomaly at RHIC. In this mechanism the baryons are product of the hadronization of the collinear two parton systems escaping from the QGP in the anomalous color states: the color anti-sextet $q\bar{q}$ system for quark jets, and the color decuplet/anti-decuplet gg system for gluon jets. To leading order in the coupling constant these two parton states can be produced via the processes $q \rightarrow |q\bar{q}\rangle_{\{\bar{6}\}}$ and $g \rightarrow |gg\rangle_{\{10\},\{\bar{10}\}}$, which are possible in the presence of the QGP due to color exchanges between the fast moving partons and the thermal partons. The $|q\bar{q}\rangle_{\{\bar{6}\}}$ and $|gg\rangle_{\{10\},\{\bar{10}\}}$ states can emerge from the $q\bar{q}$ and gg systems originally produced either via the vacuum (DGLAP) or induced gluon emission [17]. After escaping from the QGP the color anomalous two parton states result in creation of color tubes attached to these systems with the same anomalous color fluxes. The breaking of these color flux tubes via the Schwinger tunnel $q\bar{q}$ creation produces the hadron systems containing baryons. For the two parton states with not very soft gluons the baryons will be produced in the hard jet fragmentation region. We will call this mechanism the color anomalous baryon fragmentation (CABF).

In the CABF the production of a baryon in the jet fragmentation is compensated by production of an anti-baryon in the small momentum QGP hadronization region. Thus one can say that the color exchanges with the QGP catalyze the baryon number flow over large rapidity gap inside jets. Physically, it is analogous to the baryon number flow in the model of baryon-anti-baryon annihilation and baryon stopping developed in [18, 19, 20, 21] (for a review, see [22]). In this model $p\bar{p}$ -annihilation at the energies about several tens of GeV is related to the diquark transition from $\{\bar{3}\}$ to $\{6\}$ color state due to gluon exchange. This mechanism gives natural explanation why in the experimentally studied energy region of $p\bar{p}$ -annihilation $\sigma_{p\bar{p}}^{ann} \propto s^{-1/2}$ [20]. The diquark transition $D_{\{\bar{3}\}} \rightarrow D_{\{6\}}$ also leads to a strong baryon stopping [21]. This mechanism explains the slow rapidity dependence $\propto \exp(-y/2)$ of the baryon stopping observed at ISR [23]. This effect cannot be explained in the standard quark-gluon string model [24, 25, 26] which treats the diquark as a point-like color anti-triplet object. In the model

[22] the dependence $\sigma_{\bar{p}p}^{ann} \propto s^{-1/2}$ is a pre-asymptotic effect, and not the real limiting behavior of the annihilation cross section. In the high energy limit the baryon number flow in $\bar{p}p$ -annihilation is related to the color decuplet double gluon exchange. It leads to the three sheet events with the energy independent cross section $\sim 1 - 2$ mb [18, 19]. The analysis of the experimental data on the difference $\Delta\sigma_n = \sigma_n^{\bar{p}p} - \sigma_n^{pp}$ between the topological cross sections at the energies 10-1500 GeV indeed shows that the annihilation cross section has a small almost energy independent component $\sigma_{ann}^{\bar{p}p} \sim 1.5$ mb [18]. From the point of view of the SJ concept the annihilation via the color decuplet gg -exchange can be regarded as a pQCD analogue of the $J\bar{J}$ -annihilation. Gotsman and Nussinov [27] have argued that due to the vector nature of the gluon field $\sigma_{J\bar{J}}^{ann}$ should be approximately energy independent, and from the purely geometrical estimates obtained $\sigma_{J\bar{J}}^{ann} \sim 1 - 2$ mb. It agrees well with the contribution of the color decuplet double gluon mechanism obtained in [18, 19]. In pQCD the energy independence of the annihilation cross section for the decuplet double gluon mechanism is also a direct consequence of the unit gluon spin. In the sense of the unitarity condition $\sigma_{J\bar{J}}^{ann} \approx \text{const}$ would correspond to the $J\bar{J}$ Regge trajectory (if it exists) with intercept $\alpha_{J\bar{J}}(0) \approx 1$. It contradicts to the Rossi and Veneziano hypothesis that $\alpha_{J\bar{J}}(0) \approx 0.5$ and that namely $J\bar{J}$ -annihilation is responsible for $\sigma_{\bar{p}p}^{ann} \propto s^{-1/2}$ at energies ~ 10 GeV. However, the Rossi-Veneziano scenario leads to several apparent contradictions [22] that have not satisfactory explanations within the topological expansion scheme [7, 8] (the interested reader is referred to [22] for details). The problems inherent to the Rossi-Veneziano scenario with $\alpha_{J\bar{J}}(0) \approx 0.5$ do not arise in the scenario with the gluon mechanism of the baryon number flow at the pre-asymptotic energies [20, 22]. From the point of view of this model the physical mechanism of the pre-asymptotic $p\bar{p}$ -annihilation lies outside the topological expansion and has nothing to do with the $J\bar{J}$ Regge trajectory. We emphasize that $p\bar{p}$ -annihilation due to the $D_{\{3\}} \rightarrow D_{\{\bar{6}\}}$ transition [20] does not contradict to the Y -shaped baryon configuration. But it shows that the corrections to the topological expansion scheme may be huge. In principle, strong deviation from the topological expansion in the high energy processes with baryons is not surprising. Indeed, in this approach the SJ is a point-like object, but the lattice simulation shows that the SJ is a highly non-local object with the size ~ 1 fm [11].

Although, the gluon mechanism of the baryon number flow [18, 19, 20, 21] was successful in explaining a variety of the experimental data on the processes with baryons, the estimates of its contribution to the baryon production in AA -collisions are still lacking. A reliable quantitative computation of the CABF can be hardly made at present. But as a first step toward understanding the potential importance of the CABF at RHIC and LHC, it would be interesting to make at least rough estimates. This is the purpose of the present paper.

The plan of the paper is as follows. In Sec. 2 we formulate our basic assumptions on the medium modification of the high- p_T hadron spectra. In Sec. 3 we discuss the physical picture of the CABF related to the parton processes $q \rightarrow |qg\rangle_{\{\bar{6}\}}$ and $g \rightarrow |gg\rangle_{\{10\},\{\bar{10}\}}$, and then give our basic formulas for the anomalous baryon fragmentation. In Sec. 4 we present the numerical results. We give conclusions in Sec. 5.

2 High- p_T hadron yields and the medium-modified fragmentation functions

Let us begin with our basic assumptions about the medium modification of the high- p_T hadron production. We assume that the differential yield of high- p_T hadrons in AA -collisions can be written in terms of the medium-modified cross section for the $N + N \rightarrow h + X$ process [28]. In analogy to the ordinary pQCD, we write it in the form

$$\frac{d\sigma_m(N + N \rightarrow h + X)}{d\mathbf{p}_T dy} = \sum_i \int_0^1 \frac{dz}{z^2} D_{h/i}^m(z, Q, L) \frac{d\sigma(N + N \rightarrow i + X)}{d\mathbf{p}_T^i dy}. \quad (2)$$

Here $\mathbf{p}_T^i = \mathbf{p}_T/z$ is the parton transverse momentum, $d\sigma(N + N \rightarrow i + X)/d\mathbf{p}_T^i dy$ is the ordinary hard cross section, and $D_{h/i}^m$ is now the medium-modified fragmentation function (FF) for transition of an initial parton i to the observed hadron h , L is the parton path length in the QGP.

As usual we assume that in AA -collisions hadronization of fast partons happens after escaping from the QGP. Under the usual assumption of independent parton fragmentation/hadronization in vacuum the $D_{h/i}^m$ can be approximated as [29]

$$D_{h/i}^m(z, Q, L) \approx \int_z^1 \frac{dz'}{z'} D_{h/j}(z/z', Q(L)) D_{j/i}^m(z', Q, L), \quad (3)$$

where there is an implicit sum over the parton species $j = q, g$, $D_{h/j}(z, Q(L))$ is the ordinary vacuum FF, and $D_{j/i}^m(z', Q, L)$ is the medium-modified FF for transition of an initial parton i with virtuality Q to a parton j escaping from the QGP. Here $Q(L)$ is the typical virtuality of the final partons at the boundary of the QGP. From the uncertainty relation $\Delta E \Delta t \gtrsim 1$ one can obtain $Q^2(L) \sim \max(Q/L, Q_0^2)$, where $Q_0 \sim 1 - 2$ GeV is some minimal nonperturbative scale. We will discuss jets with energy up to several tens of GeV. For RHIC and LHC conditions the lifetime/size of the QGP is about the nucleus radius, R_A . For $L \sim R_A \sim 6$ fm from the above formula one can see that for parton energy $E \lesssim 100$ GeV the fragmentation/hadronization scale turns out to be relatively small $\mu_h \sim Q(L) \sim Q_0$. For such a virtuality scale the parton fragmentation outside the QGP can be described as hadronization of the color flux tubes/strings attached to the fast partons [30, 24, 25, 26], which comes through sequential breaking of the color flux tubes via the Schwinger tunnel production of $q\bar{q}$ pairs.

The medium-modified FF $D_{j/i}^m(z, Q, L)$ accumulates both the ordinary vacuum (DGLAP) gluon emission and the induced gluon radiation due to multiple scattering in the QGP. In general, one cannot separate the DGLAP and the induced stages since at least part of the DGLAP shower occurs in the medium. However, in the parton energy region $E \lesssim 100$ GeV the effect of the overlapping of these two stages should not be strong. The point is that at such energies almost all the DGLAP gluon emission occurs at the length/time scale $\lesssim 0.3 - 1$ fm [29]. It is of the order of the QGP formation time $\tau_0 \sim 0.5$ fm. For this reason in a first approximation one can neglect the overlapping of the DGLAP region with the medium. Then taking advantage of the fact that the induced gluon emission occurs mostly after the DGLAP stage, in the length range approximately

from τ_0 to R_A , one can write approximately the medium-modified FF $D_{j/i}^m$ as a convolution [29]

$$D_{j/i}^m(z, Q, L) \approx \int_z^1 \frac{dz'}{z'} D_{j/l}^{ind}(z/z', E_l, L) D_{l/i}^{DGLAP}(z', Q), \quad (4)$$

where $E_l = Qz'$, $D_{j/l}^{ind}$ is the induced FF for parton transition $l \rightarrow j$ in the QGP (it depends on the parton energy E , but not the virtuality), and $D_{l/i}^{DGLAP}$ is the ordinary DGLAP partonic FF.

In the above physical picture with independent parton fragmentation the major medium effect is a shift of the variable z in $D_{j/i}^m(z, Q, L)$ in (4) as compared to the variable z' in the DGLAP FF in (4) due to the induced parton energy loss described by the $D_{j/l}^{ind}$ FF. This leads to suppression of the hadron spectra in AA -collisions (usually called the jet quenching). Because the hard cross sections are steeply falling functions of p_T the jet quenching is mostly controlled by the induced FFs at z very close to unity [28]. For the baryon/meson ratios the parton energy loss is not very important. It can give only a small effect due to the difference in the quark and gluon suppressions and FFs to baryons. We will not consider this effect.

3 The collinear $|qq\rangle_{\{\bar{6}\}}$ and $|gg\rangle_{\{10\},\{\bar{10}\}}$ states and the anomalous baryon production

The shift of the parton longitudinal momenta related to the induced gluon emission is not the only medium effect in jet production in AA -collisions. Due to the color exchanges between the fast moving partons and the QGP the parton system after escaping from the plasma may turn out to be in the anomalous (forbidden in the vacuum) color states. We will consider only the two parton almost collinear qq and gg final states for quark and gluon jets, respectively. In vacuum the qq system is always in the $\{3\}$ color state, and the gg system in the $\{8_f\}$ color state. However, after color exchanges with the QGP as shown in Fig. 1 the qq system can be in the $\{3\}$, $\{\bar{6}\}$ and $\{15\}$ color states, and the gg system in the $\{1\}$, $\{8_f\}$, $\{8_d\}$, $\{10\}$, $\{\bar{10}\}$, and $\{27\}$ color states¹. These new color states, which are absent for jets in the vacuum, can violate the independence of the parton fragmentation, and the formulas (2), (3) will not be valid anymore. In principle, the collinear two parton configuration should violate the independence of the parton fragmentation even in the vacuum (i.e., for hadron-hadron collisions) in the string stage of hadronization. However, there such effects can effectively be included to the phenomenological FFs at low virtuality scale. But this does not work for AA -collisions when we have the new color states that are simply absent for the vacuum fragmentation (if one neglects the higher-twist interactions between comovers), and such states should be taken into account separately.

There is a set of new jet color chemistry phenomena related to production of the anomalous color states. The change of the total jet color charge may be important in

¹In principle, for a non-local parton system one needs to fix a point where the color representation is defined and introduce the Wilson lines connecting the partons with this point (similarly to the formula (1)). However, in the perturbation theory (in a gauge with gluon field vanishing at large distances, say, in Feynman gauge) this complication does not arise since the Wilson line factors can be replaced by unity.

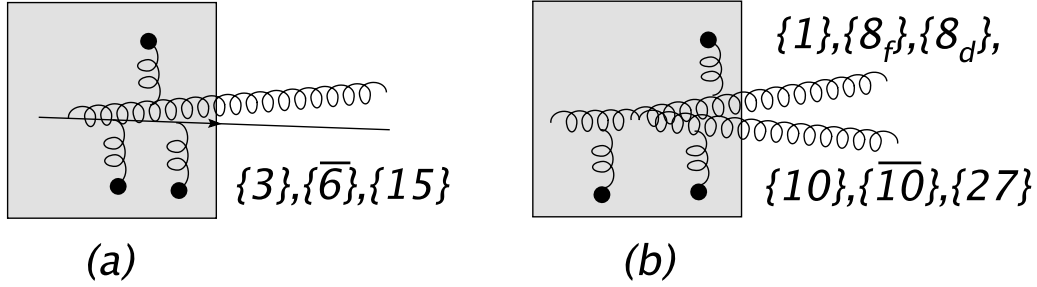


Figure 1: The $q \rightarrow gq$ (a) and $g \rightarrow gg$ (b) transitions in the medium and possible color states of the final two parton systems.

the aspect of the large angle soft gluon emission which is sensitive namely to the total jet color charge. Evidently the appearance of the higher color states should increase the multiplicity in the fragmentation region as well. This effect is similar to the modification of the parton branchings due to color exchanges with the medium discussed recently in [31] from the point of view of the large- N_c limit. On the other hand, the appearance of the color singlet gg state may lead to jet events of the diffractive type with a rapidity gap between the bulk of soft hadrons and a fast moving meson system. The effect may be enhanced for η and η' mesons (or glueballs) due to the two-gluon Fock component in their wave functions [32]. In principle, the experimental analysis of such events would be of interest for the glueballs search. And what is interesting to us is that the production of the $\{\bar{6}\}$ qq state and $\{10\}$, $\{\bar{10}\}$ gg states can be a source of the CABF since, as was noted in the Introduction, these two parton states can create the color strings decaying into hadron systems with a leading baryon (or an anti-baryon for the $\{10\}$ gg state).

3.1 Basic concepts of the model

Let us consider the CABF related to the collinear $|qq\rangle_{\{\bar{6}\}}$ and $|gg\rangle_{\{10\},\{\bar{10}\}}$ configurations. After escaping from the QGP there will be formed the sextet and decuplet color flux tubes attached to these states. The color neutralization of the sextet color tube formed by the $|qq\rangle_{\{\bar{6}\}}$ system occurs through the tunnel creation from the vacuum of two $q\bar{q}$ pairs (since the sextet color wave function is a tensor Ψ_{ij} with two color spinor indices). It results in formation of the color singlet primary heavy tube/prehadron state of unit baryon number. In Fig. 2a such a state is shown in terms of the elementary strings with triplet color flux and SJ. The hard gluon as in the Lund model [26] is represented by a kink in the color string. Similarly, for the $|gg\rangle_{\{10\},\{\bar{10}\}}$ systems the color neutralization of the decuplet color flux tubes occurs via tunnel production of three $q\bar{q}$ pairs (since the decuplet color wave function is a tensor Ψ_{ijk} with three color spinor indices)². For the $|gg\rangle_{\{\bar{10}\}}$ state it results

²In principle, for the decuplet states the color neutralization of the decuplet flux tube can go through the tunnel production of two gg pairs. However, the tunnel gluon production should be strongly suppressed due to large effective gluon mass in the QCD vacuum, and it is usually neglected in the quark-gluon string models.

in formation of a prehadron state with the baryon number $B = 1$ shown in Fig. 2b, and for the $|gg\rangle_{\{10\}}$ state a prehadron with $B = -1$. Of course, for formation of the prehadron states shown in Fig. 2 the parent two parton states should be collinear enough. We will discuss the corresponding conditions below. The hadronization of the primary prehadrons shown in Fig. 2 via sequential decays should result in production of baryons in the jet fragmentation region.

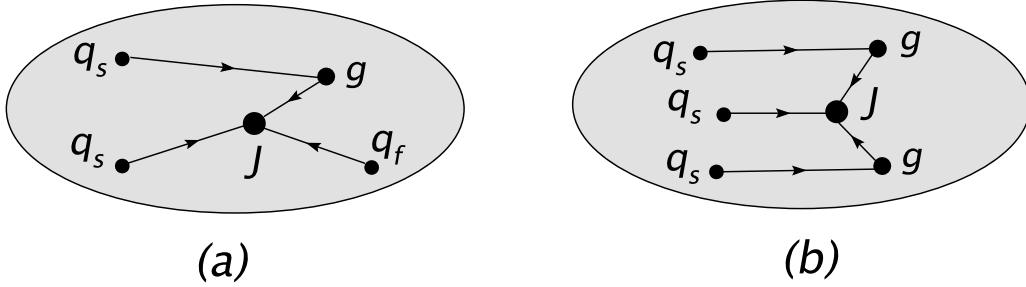


Figure 2: The primary heavy color flux tubes created by the $|qg\rangle_{\{\bar{6}\}}$ (a) and $|gg\rangle_{\{\bar{10}\}}$ (b) systems after color neutralization via the $q\bar{q}$ pairs production, q_s and q_f are the low energy (created through the Schwinger tunnel mechanism) and high energy quarks, respectively. J denotes the SJ.

An accurate description of the fragmentation of the color flux tubes formed by the $|qg\rangle_{\{\bar{6}\}}$ and $|gg\rangle_{\{10\},\{\bar{10}\}}$ configurations is an extremely difficult problem. We assume that the hadronization of the primary prehadrons shown in Fig. 2 can be described as independent hadronization of the color string configurations shown in Fig. 2. Similarly to the Lund model [26], the hard gluon kinks in the primary prehadron states in Fig. 2 are assumed to split into the collinear $q\bar{q}$ pairs with the pQCD z -distribution $W(z) \propto P_{qG}(z) \propto [z^2 + (1-z)^2]$ (here z is the quark fractional momentum). In numerical calculations we neglect the gluon splitting into strange quarks. After the $g \rightarrow \bar{q}q$ splitting the primary prehadron states shown in Fig. 2 take the forms shown in Fig. 3.

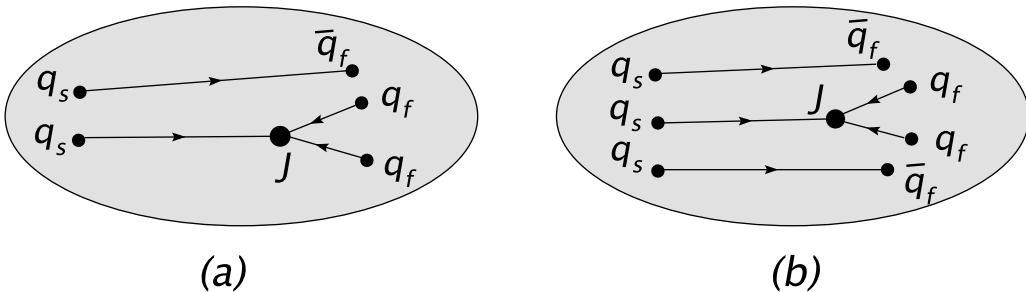


Figure 3: The same as in Fig. 2 after gluon splitting into $q\bar{q}$.

In the approximation of independent hadronization of the color strings we can express

the CABF corresponding to the configurations in Fig. 3 in terms of the diquark fragmentation function $D_{B/D}$ for the color anti-triplet diquark $D_{\{\bar{3}\}}$ (for clarity we will omit the color index $\{\bar{3}\}$). It allows one to use as much as possible the information on the diquark fragmentation extracted from fitting the baryon spectra in hadron collisions within the quark-gluon string model [24, 25]. The independence of the hadronization processes for the elementary color strings is the basic idea of the quark-gluon string model [24, 25]. It is based on the topological expansion [9] scheme (for processes without baryons the leading terms of the topological expansion are equivalent to the leading order terms in the expansion in $1/N$ ($N = N_c$, $N_c/N_f = \text{const}$ [33])). For the processes with baryons which include the string configurations with the SJ the topological expansion has not been rigorously established. But the idea that the triplet color strings should hadronize independently for the configurations with the SJ as well is credible, and we use it as a reasonable working hypothesis for qualitative estimates of the CABF. We emphasize that the physical picture shown in Figs. 2, 3 in terms of the elementary triplet color strings is not crucial for the fact that the $|qq\rangle_{\{\bar{6}\}}$ and $|gg\rangle_{\{\bar{10}\}}$ states should produce the leading baryons. Indeed, the recent lattice simulation of the color flux tubes performed in [34] demonstrates that the string tension for the triplet, sextet and decuplet color flux tubes is roughly proportional to the number of the spinor color indices for the corresponding color representations. For this reason one can expect that without reference to the strings with the triplet color flow the $q\bar{q}$ pair creation rates (which controls the resulting baryon z -distribution) for the sextet and decuplet color flux tubes should be approximately the same as for independent hadronization of the elementary triplet strings.

Analytically in our approximation the anomalous baryon FF $D_{B/i}^m$, which should be used in (2), can be written as

$$D_{B/i}^m(z, Q, L) \approx \int_z^1 \frac{dz'}{z'} D_{B/D}(z/z') D_{D/i}(z', Q, L) \quad (5)$$

with $D_{D/i}(z, Q, L)$ being the probability distribution to find in the color anomalous two parton system created by the parent parton i with the virtuality Q the diquark D with fractional momentum z (immediately after escaping from the QGP). The formula (5) is the analogue to (3) written for a single parton under the approximation of independent parton fragmentation. Note that for our $|qq\rangle_{\{\bar{6}\}}$ and $|gg\rangle_{\{\bar{10}\}}$ configurations the diquark is automatically in the anti-triplet color state. In our numerical computations we use the parametrization of the diquark to proton fragmentation function of the form $D_{p/D}(z) = Az^m$ with $m = 5/2$ obtained in fitting the proton spectra in hadron reactions within the quark-gluon string model in [35].

In calculating the $D_{D/i}$ we treat the diquark as being consisting of the two fastest quarks in the prehadrons shown in Fig. 3. It is a natural assumption since for the CABF we are interested in the hard region with z close to unity. Then we can calculate the diquark distribution treating perturbatively the creation of the $|qq\rangle_{\{\bar{6}\}}$ and $|gg\rangle_{\{\bar{10}\}}$ configurations. We calculate the diquark distribution describing the diquark as a two quark configuration with some invariant mass cutoff M_D . We will perform calculations for $M_D = 1$ and $M_D = 1.5$ GeV. These values seem to be reasonable in the light of the calculations of the diquark masses within the Dyson-Schwinger equation which give the diquark masses $\sim 0.8 - 1$ GeV [36, 37]. Since we work with non-interacting quarks our parameter M_D

may be somewhat bigger than the real diquark mass. For this reason the value $M_D = 1.5$ does not look unrealistic. Note that the mass cutoff at $M_D \sim m_N$ ensures that the baryon production is not accompanied by production of the leading mesons with the fractional momentum $z \sim 1$. These mesons should inevitably shift the baryon distribution to the low- z region which is not important from the point of view of the high- p_T baryon yield. We will denote the diquark FF with this mass cutoff $D_{D/i}(z, M_D)$ (hereafter we suppress the arguments Q and L).

We emphasize that although the configurations with $M_D \gg m_N$ are not important for the baryon/meson ratios they, of course, also lead to the CABF. Such configurations should enhance the baryon FFs in AA -collisions as compared to the ordinary baryon FFs at $z \ll 1$. The states with $M_D \gg m_N$ are produced when the radiated gluons in Fig. 1 are very soft. For the induced gluon radiation, which dominates the CABF for RHIC and LHC conditions, most of the gluons have energies $\lesssim 5$ GeV. After the $g \rightarrow \bar{q}q$ splitting the typical energy of the softest quarks in the $q_f q_f$ systems in the primary prehadron states in Fig. 3 will lie in the same energy range. For the very asymmetric $q_f q_f$ configurations the SJ should have a rapidity close to that for the softest quark in the $q_f q_f$ pair (since it minimizes the string energy). It will result in production of a baryon with energy about the typical energy of the emitted gluons in Fig. 1, i.e., in the soft region $z \ll 1$. The hadronization of the strings attached to the fastest quarks in the asymmetric $q_f q_f$ pairs in Fig. 3, which controls the FFs in the hard region $z \sim 1$, should be similar to that for the ordinary vacuum fragmentation. In the present paper we concentrate namely on the role of the CABF in the baryon/meson ratios and will not consider the effect of the CABF on the FFs in the soft region.

3.2 Calculation of the diquark distribution

The main ingredient in our model for the CABF is the diquark distribution $D_{D/i}$. We illustrate its calculation for a quark jet. For pure two parton gq state, i.e. for $q \rightarrow |gq\rangle_{\{\bar{6}\}}$ transition without multiple gluon emission we write $D_{D/q}$ as

$$D_{D/q}(z, M_D) = \int_0^1 dx dy \frac{dN_{gq}^{\{\bar{6}\}}}{dx} W(y) \delta(z - z_D) \theta(M_D - M_{q_1 q_2}). \quad (6)$$

Here $dN_{gq}^{\{\bar{6}\}}/dx$ is the gluon distribution for the $q \rightarrow |gq\rangle_{\{\bar{6}\}}$ transition, with $x = p_g/p_q$ being the fractional gluon momentum, y is the quark fractional momentum for $g \rightarrow \bar{q}q$ splitting, $z_D = 1 - x + xy$ is the total fractional momentum of the fast quarks (we denote the quark which radiates the gluon q_1 and the quark from the $g \rightarrow \bar{q}q$ splitting q_2), and $M_{q_1 q_2}$ is the invariant mass for the $q_1 q_2$ system.

For the sake of simplicity we account for the transverse (to the jet axis) motion effects on the average, so to speak, via the effective transverse quark mass m_T and approximate $M_{q_1 q_2}$ by a one-dimensional formula

$$M_{q_1 q_2}^2 = \frac{m_T^2}{z_1} + \frac{m_T^2}{z_2}, \quad (7)$$

where $z_1 = (1 - x)/z_D$, $z_2 = xy/z_D$ are the fractional momenta of the quarks in terms of the x and y variables. Our choice of m_T will be given below in Sec. 4.

The distribution function $dN_{gq}^{\{\bar{6}\}}/dx$ in (6) corresponds to the final $|gq\rangle_{\{\bar{6}\}}$ state escaping from the QGP. The gluon in this state can be originally produced either in the DGLAP stage due to the vacuum $q \rightarrow gq$ transition without interaction with the medium or in the bulk QGP via the induced gluon emission. The distribution $dN_{gq}^{\{\bar{6}\}}/dx$ should be calculated including both these mechanisms. We will refer to them as the DGLAP and induced mechanisms. We emphasize that in our case both of them are the medium effects. Even for the DGLAP mechanism when the initial gq system is produced in the triplet color state the final $|gq\rangle_{\{\bar{6}\}}$ state escaping from the QGP emerges only due the subsequent color exchanges between the gq system and the medium.

Let us now consider the incorporation of the multiple gluon emission, which is neglected in the formula (6). The radiation of additional gluons can occur in the DGLAP stage (as was already noticed mostly at the longitudinal scale ~ 1 fm) and in the subsequent induced gluon radiation stage in the whole volume of the QGP. An accurate description of the multiple gluon emission is a complicated problem. However, it can be made in a reasonable approximation, which is sufficient for our purposes here. To incorporate the multiple gluon emission we use the fact that the CABF is dominated by a region of moderate x around $x \sim 0.5$ (since only for such configuration a hard and not very heavy diquark can be produced). On the other hand, both the DGLAP and especially induced multiple gluon radiation are mostly soft with $x \ll 1$. Thus the collinear two parton system determining the CABF and the soft gluons act, so to speak, in the different regions of the phase space. For soft gluons the two parton collinear gq state with hard gluon should approximately act as a single fast quark. For this reason the effect of the Sudakov formfactor (related to the virtual gluons) and real gluon emission for the gq state should roughly be similar to that for a single quark.

For a single quark the DGLAP and induced radiation lead simply to replacement of the hard parton cross section by

$$\frac{d\sigma_{eff}(N + N \rightarrow j + X)}{d\mathbf{p}_T^j dy} = \sum_i \int_0^1 \frac{dz}{z^2} D_{j/i}^{ind}(z, p_T^i, L) \times \frac{d\sigma_{DGLAP}(N + N \rightarrow i + X)}{d\mathbf{p}_T^i dy}, \quad (8)$$

where

$$\frac{d\sigma_{DGLAP}(N + N \rightarrow j + X)}{d\mathbf{p}_T^j dy} = \sum_i \int_0^1 \frac{dz}{z^2} D_{j/i}^{DGLAP}(z, Q) \frac{d\sigma(N + N \rightarrow i + X)}{d\mathbf{p}_T^i dy}. \quad (9)$$

Here, as in (4), $D_{j/i}^{ind}$ and $D_{j/i}^{DGLAP}$ denote the induced and DGLAP partonic FFs, and $p_T^i = p_T^j/z$. This representation is written taking into account the time ordering of the DGLAP and the induced radiation stages. Thus we can work with the formula (6) for pure two parton gq state but at the same time we should replace the LO pQCD cross section by that given by Eq. (8). In fact, for the baryon/meson ratio one can go one step further in simplification of the calculations. It is based on the fact that the ratio $\sigma_{eff}/\sigma_{DGLAP}$ is close to the nuclear modification factor R_{AA} for the meson cross section. For this reason it is enough to replace the LO pQCD hard cross section by the σ_{DGLAP} (9), and at the same time to use for the denominator in the baryon/meson ratio the meson cross section for NN -collisions.

We are fully aware that the above procedure does not treat accurately the real and virtual multiple gluon emission in the hard region itself. However, for the vacuum and

induced $q \rightarrow gq$ distributions the integral probability to find the gluon in the hard region (say, $x \gtrsim 0.2$ which dominates the CABF) turns out to be smaller than unity. This says that the unitarity effects related to the real and virtual multiple gluon emission are relatively small, and the difference between these effects for a single quark and the gq state cannot give large errors. In any case, presently, even for a single quark, there is no an accurate method for evaluation of the multiple induced gluon emission.

3.2.1 Calculation of $dN_{gq}^{\{\bar{6}\}}/dx$

An accurate computation of $dN_{gq}^{\{\bar{6}\}}/dx$ even at one gluon level is a difficult problem. As already noticed above, it should take into account the vacuum and induced $q \rightarrow gq$ transitions. It is important that for both these mechanisms the original gq state is subjected to rotation in the color space due to multiple gluon exchanges with the medium. Qualitative estimates show that for RHIC and LHC conditions the two parton system almost surely changes its color state in the QGP for jet energies $E \lesssim 30 - 50$ GeV. For this reason in this energy range one can expect that multiple rescatterings should result in almost complete color randomization of the two parton system. Then the probability of the $\{\bar{6}\}$ color state is simply given by the statistical weight factor $6/24$.

Let us first consider the distribution $dN_{gq}^{\{\bar{6}\}}/dx$ for the vacuum (DGLAP) creation of the gq system, i.e., without interaction with the medium. We write the leading order (x, \mathbf{q}) -distribution (hereafter \mathbf{q} denotes the momentum transverse to the jet axis) for the vacuum $q \rightarrow gq$ transition in the form

$$\frac{dN_{vac}}{dx d\mathbf{q}} = \frac{C_F \alpha_s}{2x\pi^2} [1 + (1-x)^2] \frac{q^2}{(q^2 + \epsilon^2)^2}. \quad (10)$$

Here C_F is the quark color Casimir factor, $\epsilon^2 = m_q^2 x^2 + m_g^2 (1-x)$, $m_{q,g}$ are the quark and gluon masses. In our numerical computations we take $m_g = 0.75$ GeV. This value was obtained from the analysis of the low- x proton structure function F_2 within the dipole BFKL equation [38]. It agrees well with the natural infrared cutoff for gluon emission $m_g \sim 1/R_c$, where $R_c \approx 0.27$ fm is the gluon correlation radius in the QCD vacuum [39]. For the quark mass we take $m_q = 0.3$ GeV. However, the value of the quark mass is not very important.

Of course, the final (after escaping from the QGP) (x, \mathbf{q}) -distribution for the gq system created in the DGLAP stage, differs from the primordial one (10) due to the transverse momentum broadening in the QGP. We write it (we denote it by a subscript br) as a convolution

$$\frac{dN_{vac}^{br}}{dx d\mathbf{q}} = \int d\mathbf{k} \frac{dN_{vac}}{dx d\mathbf{k}} I_{br}(\mathbf{q} - \mathbf{k}), \quad (11)$$

where $I_{br}(\mathbf{q})$ is the distribution for the broadening in the internal transverse momentum of the gq system. The internal transverse momentum in terms of the gluon and quark momenta reads $\mathbf{q} = (1-x)\mathbf{q}_g - x\mathbf{q}_q$. We treat the \mathbf{q} -broadening as an independent random walk of the quark and gluon in transverse momenta characterized by their transport coefficients [40, 17]. Then the $I(\mathbf{q})$ has a Gaussian form

$$I_{br}(\mathbf{q}) = \frac{1}{\pi \langle \mathbf{q}^2 \rangle} \exp\left(-\frac{\mathbf{q}^2}{\langle \mathbf{q}^2 \rangle}\right), \quad (12)$$

$$\langle \mathbf{q}^2 \rangle = \int_{\tau_0}^L dl [(1-x)^2 \hat{q}_g(l) + x^2 \hat{q}_q(l)], \quad (13)$$

where $\hat{q}_g(l)$ and $\hat{q}_q(l)$ are the local gluon and quark transport coefficients related by $\hat{q}_g(l) = \hat{q}_q(l)C_A/C_F$. In (13) we have taken for the lower limit of the l -integral the QGP formation time τ_0 since the typical gluon formation time for the vacuum $q \rightarrow gq$ transition is of the order of τ_0 , and the gq system should undergo scattering on the thermal partons immediately after formation of the QGP. In any case, the corresponding inaccuracy cannot be big since the resulting $\langle \mathbf{q}^2 \rangle$ has only weak logarithmic dependence on the limits of the l -integration.

We write the resulting vacuum contribution to $dN_{gq}^{\{\bar{6}\}}/dx$ as

$$\left. \frac{dN_{gq}^{\{\bar{6}\}}}{dx} \right|_{vac} = A_{\{\bar{6}\}} \int_{q < q_{max}} d\mathbf{q} \frac{dN_{vac}^{br}}{dx d\mathbf{q}}, \quad (14)$$

where we introduced the color weight factor $A_{\{\bar{6}\}} = 6/24$ of the anti-sextet state. The restriction $q < q_{max}$ is imposed to cut off the non-collinear configurations which cannot produce the prehadron state with two fast quarks located in the same cavity in the terminology of the MIT bag-model. For the transverse size of the prehadron cavity it is reasonable to use the proton radius $R_p \sim 1$ fm (this value is also consistent with the transverse size of the sextet and decuplet color tubes about 0.8 fm obtained in the lattice simulation [34]). Then for the parton energy $\sim 10-20$ GeV one can obtain $q_{max} \lesssim 0.3-0.5$ GeV (we assume that for the radiated gluon $x \sim 0.5$ and the size of the QGP is about 5 fm). Note that this transverse momentum region is reasonable from the point of view of the diquark mass as well, since it leads to $M_D \lesssim 1-2$ GeV. A larger value of q_{max} (which is possible from the geometrical viewpoint at higher energies) would give too heavy diquark which should have a smaller probability for fragmentation into a leading baryon.

Let us now discuss the induced contribution to $dN_{gq}^{\{\bar{6}\}}/dx$. An accurate evaluation of the (x, \mathbf{q}) -distribution for the induced gluon emission (necessary for calculation of the x -distribution) even at one gluon level is problematic. In principle, the (x, \mathbf{q}) -spectrum can be computed within the light-cone path integral (LCPI) formalism [41, 42]. However, it requires solving a complicated two dimensional Schrödinger equation with a non-central potential. In the present qualitative analysis, to avoid this complications, we use the LCPI formalism only for calculation of the transverse momentum integrated spectrum dN_{ind}/dx , and parametrize the transverse momentum dependence in a Gaussian form. We assume that the mean squared momentum can be approximated as a sum

$$\langle \mathbf{q}^2 \rangle = \langle \mathbf{q}^2 \rangle_{fz} + \langle \mathbf{q}^2 \rangle_{ms}, \quad (15)$$

where the first term corresponds to the primordial internal momentum of the gq system in the gluon formation zone and the second one comes from the momentum accumulated due to multiple scatterings. The formation zone term can be written via the mean squared transverse separation between gluon and quark as $\langle \mathbf{q}^2 \rangle_{fz} \sim 4/\langle \rho_{gq}^2 \rangle$. From the Schrödinger diffusion relation one can obtain $\langle \rho_{gq}^2 \rangle \sim 2L_{typ}/x(1-x)E$. Here $L_{typ} = \max(L_{QGP}, L_f)$, where L_f is the gluon formation length. For induced radiation the gluon formation length is approximately $L_f \sim 2x(1-x)ES_{LPM}/\epsilon_{pl}^2$ [42], where S_{LPM} is the Landau-Pomeranchuk-Migdal (LPM) suppression factor, the index pl of ϵ_{pl} indicates that it should be calculated

with parton masses replaced by the corresponding quasiparticle masses in the plasma. We use the quasiparticle masses $m_q = 0.3$ and $m_g = 0.4$ GeV obtained within the quasiparticle model of the QGP in [43]. The LPM suppression for RHIC and LHC conditions is not very strong. Typically the LPM effect suppresses the gluon spectrum by a factor $\sim 1.5 - 3$. For moderate x , important for the CABF, and parton energy region $E \sim 5 - 30$ the L_f turns out to be of the order of the plasma size or even larger. This says that, strictly speaking, one cannot separate the effects of the primordial internal momentum in the gluon formation zone and that due to multiple scatterings. However, for our rough estimates it is not very important since numerically the effect of the primordial momentum is relatively small, and the width of the transverse momentum distribution is mostly controlled by multiple scatterings.

Note that in our treatment of the \mathbf{q} -broadening (both for the vacuum and induced gg states) we neglected the contribution of the transverse momentum kicks related to the soft gluon emission. An accurate evaluation of this effect is complicated. However, it should not change drastically our results. First of all, the number of elastic kicks is considerably larger than that from the radiated soft gluons. Also, the kicks from the soft gluon emission mostly occur before the formation of the gg system with a hard gluon (since the gluon formation length is $\propto x$) and do not affect the \mathbf{q} -distribution at all. This is especially true for the induced mechanism, for which multiple gluon emission is very soft. As will be seen from our numerical results namely the induced mechanism dominates the CABF.

In connection with Eq. (6) it is perhaps worth noting that although for the dominating induced mechanism the x -distribution $dN_{gg}^{\{6\}}/dx$ is concentrated in a sharp peak at small x with a width $\propto 1/E$ it does not generate a strong energy dependence of the CABF. The strong energy dependence could naively be expected from the decrease with the jet energy of the overlap of the region with $M_D \lesssim m_N$ with the low- x peak in $dN_{gg}^{\{6\}}/dx$. In reality, the low- x peak in the gluon distribution is practically not important for the baryon yield for $p_T \gtrsim 5 - 10$ GeV. Our numerical calculations show that in the region $x \gtrsim 0.2 - 0.3$, which dominates the CABF for $M_D \sim m_N$, the distribution $dN_{gg}^{\{6\}}/dx$ already has a quite smooth x -dependence (approximately $\propto 1/x^\alpha$ with $\alpha \sim 1 - 1.5$ for the jet energy $E \sim 5 - 50$ GeV). The same is true for the $dN_{gg}^{\{10\}}/dx$ entering Eq. (16) for the gluon jets. As already noticed above, the low- x peak in the gluon distribution is, of course, important for the enhancement of the baryon FFs in the the soft region $z \ll 1$. This effect, related to the very asymmetric $q_f q_f$ configuration in Fig. 3, is not described by Eqs. (6) and (16). But the baryon yield at high p_T , which we are interested in, is practically insensitive to the baryon FFs at small z .

3.2.2 The gluon jets

The baryon production for gluon jet is treated in a similar way as a three-step process that now involves first the production of the gg pair in the decuplet/anti-decuplet color state, followed by the diquark formation (after splitting of hard gluons into $q\bar{q}$ pairs and formation of the configuration shown in Fig. 3b), and final diquark fragmentation to the

observed baryon. The analog of Eq. (6) for the state shown in Fig. 3b has the form

$$D_{D/g}(z, M_D) = \frac{1}{2!} \int_0^1 dx dy_1 dy_2 \frac{dN_{gg}^{\{\overline{10}\}}}{dx} W(y_1) W(y_2) \delta(z - z_D) \theta(M_D - M_{q_1 q_2}), \quad (16)$$

where now $z_D = (1-x)y_1 + xy_2$, the factor $1/2!$ accounts for the gluon identity, and the light-cone fractional momenta in the formula (7) for the invariant mass $M_{q_1 q_2}$ read $z_1 = (1-x)y_1/z_D$ and $z_2 = xy_2/z_D$. Similarly to the quark case, for the (x, \mathbf{q}) -distribution for the vacuum $g \rightarrow gg$ transition we use the leading order formula

$$\frac{dN_{vac}}{dx d\mathbf{q}} = \frac{C_A \alpha_s}{\pi^2} \left[\frac{1-x}{x} + \frac{x}{1-x} + x(1-x) \right] \frac{q^2}{(q^2 + \epsilon^2)^2}, \quad (17)$$

where now C_A is the gluon color Casimir factor, and $\epsilon^2 = m_g^2(1-x+x^2)$. The statistical weight factor for the $\{\overline{10}\}$ color state is now $A_{\{10\}} = 10/64$.

3.2.3 The energy dependence beyond the color randomization approximation

We conclude this section with a general comment about the validity region of the color randomization approximation and possible energy dependence of the CABF above the color randomization window. In the approximation of color randomization the diquark distribution $D_{D/i}$ has a weak energy dependence. However, the CABF is in general a higher-twist effect and is expected to have disappeared in the limit of high parton energies. This phenomenon is realized in the following way. For a given maximal internal momentum q_{max} the transverse separation between partons in the two parton system vanishes $\propto 1/E$ at $E \rightarrow \infty$. Since for the small size two parton states the probability of changing the color state is proportional to the size squared, the probability of production of the sextet gq and decuplet/anti-decuplet gg states should vanish $\propto 1/E^2$ in the high energy limit. This says that the approximation of the color randomization should be violated at sufficiently high energies. Our qualitative estimates show that for $E \lesssim 20 - 30$ GeV the approximation of color randomization should still be reasonable. And then in this region the higher-twist nature of the CABF should not manifest itself. Of course, one cannot exclude that the window of the color randomization may turn out to be narrower and the dynamical effects lead to some energy dependence of the weight of the $\{\overline{6}\}$ and $\{10\}/\{\overline{10}\}$ states even at $E \sim 10 - 30$ GeV. But they should not change drastically the magnitude of the CABF in this energy region.

In principle, the energy dependence of the color anomalous two parton configurations can be evaluated in the dynamical approach based on the evolution operator for the density matrix for the two parton states [44, 45]. However, our aim here is only to understand the potential importance of the CABF, and it is outside the scope of this paper to study accurately its energy dependence.

4 Numerical results

We performed the computations of the vacuum two parton distributions (10), (17) with the running α_s frozen at the value $\alpha_s^{fr} = 0.7$. This value was previously obtained by

fitting the data on nuclear shadowing [46] and proton structure function F_2 at low x within the dipole BFKL equation [38]. A similar value of α_s^{fr} follows from the relation $\int_0^2 \text{GeV} dQ \frac{\alpha_s(Q^2)}{\pi} \approx 0.36 \text{ GeV}$ obtained in [47] from the analysis of the heavy quark energy loss in vacuum. We calculate the hard parton cross sections using the LO pQCD formula. To simulate the higher order K -factor we take for the virtuality scale in α_s the value cQ with $c = 0.265$ as in the PYTHIA event generator [48].

The DGLAP parton FFs entering (9) were computed with the help of the PYTHIA event generator [48]. The x -distribution for the induced gluon emission has been computed within the LCPI formalism [41] using the method elaborated in [49]. In computing the induced gluon emission we use the running α_s frozen at the value $\alpha_s^{fr} = 0.6$. The suppression of the in-medium α_s^{fr} , which may be due to the thermal effects, is supported by the analysis of the RHIC and LHC data on the nuclear modification factor R_{AA} [29, 50].

We approximate the effective transverse quark mass entering (7) as $m_T = \sqrt{m_q^2 + \langle p_q^2 \rangle}$, where $\langle p_q^2 \rangle$ is the mean squared quark transverse momentum. We estimated $\langle p_q^2 \rangle$ for the configurations in which all the gluon momentum in the $g \rightarrow q\bar{q}$ splitting is transferred to the quark (such configurations dominates the CABF). Then a reasonable estimate is $\langle p_q^2 \rangle \approx q_{max}^2/2$.

We calculated the p/π^+ and \bar{p}/π^- ratios for the central $Au + Au$ collisions at $\sqrt{s} = 200$ GeV at RHIC, and for the $Pb + Pb$ central collisions at $\sqrt{s} = 2.76$ TeV at LHC. The \mathbf{q} -broadening has been calculated using the Bjorken model [51] of the QGP evolution with $T_0^3 \tau_0 = T^3 \tau$. We take $\tau_0 = 0.5$ fm, and $T_0 = 300$ MeV for RHIC, and $T_0 = 400$ MeV for LHC. These initial temperatures were obtained using the entropy/multiplicity ratio $dS/dy/dN_{ch}/d\eta = 7.67$ from [52]. In calculating the \mathbf{q} -broadening for the typical parton path length in the QGP in Eq. (13) we take $L = 5$ fm which is a reasonable value for the central collisions [49]. For the multiple scattering term $\langle \mathbf{q}^2 \rangle_{ms}$ in the \mathbf{q} -broadening formula (15) for the induced mechanism we take for the minimal length $L_{min} = 2$ fm (instead of τ_0 as in Eq. (13) for the vacuum mechanism). It is done to account for the fact that for the induced mechanism the gluon radiation is distributed in the region of the size $\sim L_f$. However, it gives a relatively small suppression of the \mathbf{q} -broadening since the dependence of $\langle \mathbf{q}^2 \rangle_{ms}$ on L_{min} is only logarithmic. For the gluon transport coefficient we take $\hat{q}_g = 0.3 \text{ GeV}^3$ at $T = 250$ MeV. This value is approximately consistent with accurate treatment of the p_T -broadening for our parametrization of α_s .

The results for p/π^+ and \bar{p}/π^- ratios obtained for $q_{max} = 0.3 \text{ GeV}$, $m_q = 0.3 \text{ GeV}$, and $M_D = 1$ and $M_D = 1.5 \text{ GeV}$ are plotted in Fig. 4. The results are shown separately for the vacuum mechanism and the induced one. One can see that the induced mechanism dominates. This is mostly due to the fact that from the beginning of the formation of the gq and gg systems their configurations are more collinear for the induced mechanism. The sensitivity to the diquark mass becomes stronger at larger p_T . From Fig. 4 we see that for RHIC the effect of the CABF is bigger than for LHC. It is determined by two facts: one is the p_T -dependence of the parton cross sections which is steeper at RHIC. The other is relative decrease of the quark yield at LHC which dominates the CABF at RHIC. Note that the fact that p/π^+ and \bar{p}/π^- ratios numerically are not small does not mean that the probability to find a proton/anti-proton in parton fragmentation is large. In fact, the baryon fraction is very small $\sim 1 - 5\%$. But for baryons the dominating values

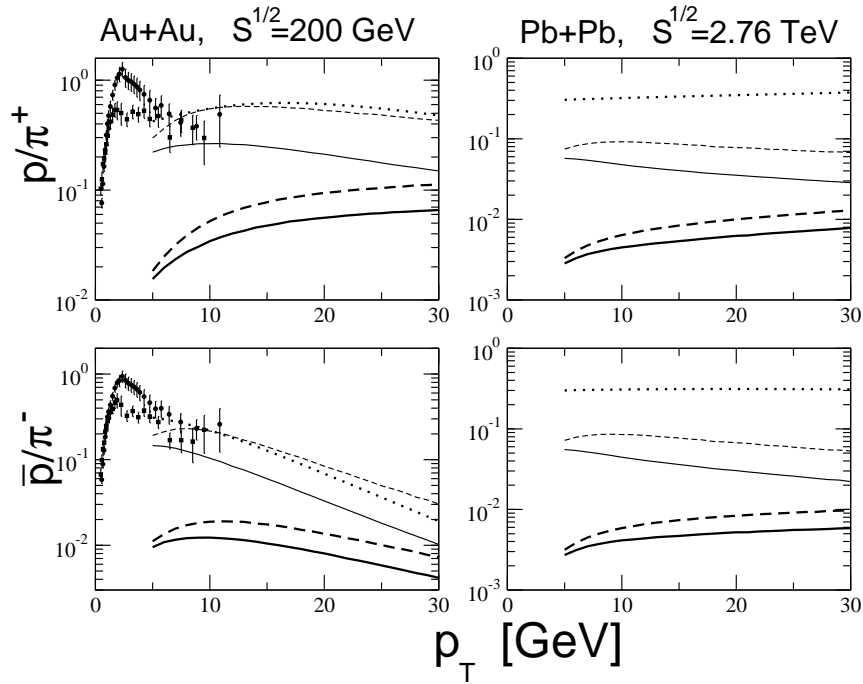


Figure 4: The p/π^+ and \bar{p}/π^- ratios for $Au + Au$ at $\sqrt{s} = 200$ GeV and $Pb + Pb$ at $\sqrt{s} = 2.76$ TeV (central collisions). The thick lines show our results for the CABF due to the gq and gg systems created in the DGLAP stage obtained for $M_D = 1$ GeV (solid) and $M_D = 1.5$ GeV (dashed), and the thin lines the same for the CABF due to the two parton systems created in the induced stage. The dotted lines show the results for NN -collisions obtained with the AKK FFs [53]. The experimental points in the left panels show the data from STAR for $Au + Au$ 0-12% central collisions [4] (circles) and $d + Au$ [55] (squares) collisions.

of z in (2) are bigger than for mesons, and due to the steep fall-off of the parton cross section it enhances strongly the numerator in the baryon/meson ratio.

The results shown in Fig. 4 have been obtained with the gluon splitting function $W(z) = 3[z^2 + (1-z)^2]/2$ which in principle has no theoretical justification for the gluon kinks in our model. To understand the sensitivity to the form of $W(z)$ we also performed the calculations for the ansatz $W(z) = 30z^2(1-z)^2$ when the quark and anti-quark have almost exactly half the gluon momentum. For this parametrization the p/π^+ and \bar{p}/π^- ratios became only $\sim 15 - 30\%$ smaller. This demonstrates that the ansatz for $W(z)$ does not play a crucial role.

To get insight into how strongly the CABF can modify the picture based on independent parton fragmentation with the ordinary vacuum FFs in Fig. 4 we also plotted the baryon/meson ratios obtained with the AKK baryon FFs [53]. As one can see for RHIC the contribution of the CABF is of the same order as that for the vacuum AKK FFs. For LHC the ratio CABF/AKK becomes somewhat smaller, but the effect of the CABF is not negligible. Thus, our estimates demonstrate that the CABF can potentially lead to a

substantial violation of the scheme based on the ordinary FFs. Note that comparing the CABF with the ordinary vacuum baryon fragmentation, one has to keep in mind that the vacuum baryon FFs themselves have considerable uncertainties. For example, the proton yield for the KKP FFs [54] is much smaller than that for the AKK FFs [53], and the relative effect of the CABF is bigger in this case.

In Fig. 4 we also plotted the STAR experimental data for $Au + Au$ [4] and $d + Au$ [55] collisions. Since the medium effects should be small for $d + Au$ collisions, the difference between the $Au + Au$ and $d + Au$ data may be attributed to the medium effects that are of interest in our analysis. As one can see at $p_T \sim 5 - 10$ GeV our estimates for the contribution of the CABF are of the same order as the difference between the data for $Au + Au$ and $d + Au$ collisions. However, the experimental errors are large and definite conclusion cannot be drawn from this comparison. At small transverse momenta $p_T \sim 2 - 3$ GeV the difference between the data for $Au + Au$ and $d + Au$ is clearly seen, and it is of the same order of magnitude as our estimates of the CABF for $p_T \sim 5$ GeV. But it can hardly be taken seriously since even at $p_T \sim 5$ GeV our approach is probably of limited applicability, and extrapolation of our results to $p_T \sim 2 - 3$ GeV would be highly speculative.

The results presented in Fig. 4 for $m_q = 0.3$ GeV can be viewed as conservative estimates. For massless quarks the effect is enhanced by a factor of $\sim 1.5 - 3$. A similar enhancement occurs for $q_{max} = 0.5$ GeV (which does not seem unrealistic). Thus, although our analysis is not expected to give accurate quantitative predictions it clearly indicates that the CABF can be potentially important at RHIC and LHC energies. And this mechanism deserves more careful investigation. In particular, it is highly desirable to perform an analysis of the CABF beyond the color randomization approximation for better understanding its energy dependence. We postpone it for further work.

5 Conclusions

Besides the well known suppression of high- p_T hadron yields in AA -collisions, the color exchanges between jets and the QGP can lead to several other new phenomena. One of these jet color chemistry effects is the anomalous contribution to the baryon yield [16]. We have estimated the anomalous baryon production due to this mechanism accounting for formation of the collinear two parton $|gq\rangle_{\{6\}}$ (for quark jets) and $|gg\rangle_{\{\overline{10}\},\{10\}}$ states (for gluon jets). The hadronization of these states can result in production of leading baryons. Conceptually this mechanism is similar to the gluon mechanism of the baryon number flow in the $B\bar{B}$ -annihilation and baryon stopping via gluon exchanges producing in a baryon/anti-baryon the two quark $qq/\bar{q}\bar{q}$ -configurations in the $\{6\}/\{\bar{6}\}$ color states and the three quark $qqq/\bar{q}\bar{q}\bar{q}$ -configurations in the $\{10\}/\{\overline{10}\}$ color states [18, 19, 20, 21].

We have estimated the contribution of our mechanism to the p/π^+ and \bar{p}/π^- ratios for the two parton anomalous states produced via the DGLAP and induced gluon emission. We found that the induced mechanism dominates. The effect is stronger for quark jets. For RHIC our estimates give the contribution to the p/π^+ and \bar{p}/π^- ratios of the same order as the ordinary vacuum fragmentation for AKK [53] FFs. At $p_T \sim 5$ the anomalous contributions to the p/π^+ and \bar{p}/π^- ratios are comparable with the medium modifica-

tion of these ratios observed by the STAR Collaboration [4]. For LHC the anomalous contribution becomes smaller than the vacuum one, but not negligible.

Of course, our estimates are extremely crude. But they indicate that the color anomalous baryon fragmentation can be potentially important at RHIC and LHC energies. Contrary to the SJ loops [5] and recombination [12, 13, 14, 15] models of the baryon anomaly the mechanism discussed in the present paper is purely of fragmentation type, and can be important at higher p_T .

Acknowledgements

The work of BGZ is supported in part by the Laboratoire International Associé "Physique Théorique et Matière Condensée" (ENS-Landau) and the grant SS-6501.2010.2.

References

- [1] M.J. Tannenbaum, Rept. Prog. Phys. **69**, 2005 (2006), and references therein.
- [2] S.S. Adler, *et al.* [PHENIX Collaboration], Phys. Rev. Lett. **91**, 172301 (2003).
- [3] J. Adams, *et al.* [STAR Collaboration], Phys. Rev. Lett. **92**, 052302 (2004).
- [4] B.I. Abelev *et al.* [STAR Collaboration], Phys. Rev. Lett. **97**, 152301 (2006).
- [5] I. Vitev and M. Gyulassy, Phys. Rev. **C65**, 041902 (2002).
- [6] V. T. Pop, M. Gyulassy, J. Barrette, C. Gale, X. N. Wang, and N. Xu, Phys. Rev. **C70**, 064906 (2004).
- [7] G.C. Rossi and G. Veneziano, Nucl. Phys. **B123**, 507 (1977).
- [8] G.C. Rossi and G. Veneziano, Phys. Rep. **63**, 149 (1980).
- [9] G. Veneziano, Phys. Lett. **B52**, 220 (1974); Nucl. Phys. **B74**, 365 (1974).
- [10] T.T. Takahashi, *et al.*, Phys. Rev. Lett. **86**, 18 (2001); T.T. Takahashi, *et al.*, Phys. Rev. **D65**, 114509 (2002).
- [11] F. Bissey, *et al.*, Phys. Rev. **D76**, 114512 (2007).
- [12] R.C. Hwa and C.B. Yang, Phys. Rev. **C67**, 064902 (2003).
- [13] R.J. Fries, B. Muller, C. Nonaka, and S.A. Bass, Phys. Rev. Lett. **90**, 202303 (2003).
- [14] V. Greco, C.M. Ko, and P. Lévai, Phys. Rev. Lett. **90**, 202302 (2003).
- [15] R.J. Fries, V. Greco, and P. Sorensen, Ann. Rev. Nucl. Part. Sci. **58**, 177 (2008) [arXiv:0807.4939 [nucl-th]].

- [16] B.G. Zakharov, Proceedings of the 33rd Rencontres de Moriond: QCD and High Energy Hadronic Interactions, Les Arcs, France, March 21-28, 1998, pp. 465-469 [arXiv:hep-ph/9807396].
- [17] R. Baier, D. Schiff, and B. G. Zakharov, Annu. Rev. Nucl. Part. Sci. **50**, 37 (2000).
- [18] B.Z. Kopeliovich and B.G. Zakharov, Phys. Lett. **B211**, 221 (1988).
- [19] B.G. Zakharov and B.Z. Kopeliovich, Sov. J. Nucl. Phys. **48**, 136 (1988).
- [20] B.G. Zakharov and B.Z. Kopeliovich, Sov. J. Nucl. Phys. **49**, 674 (1989).
- [21] B.Z. Kopeliovich and B.G. Zakharov, Z. Phys. **C43**, 241 (1989).
- [22] B.G. Zakharov and B.Z. Kopeliovich, Sov. J. Part. Nucl. **22**, 67 (1991).
- [23] B. Aper *et al.*, Nucl. Phys. **B100**, 237 (1975); T. Akesson *et al.*, Nucl. Phys. **B228**, 409 (1983).
- [24] A.B. Kaidalov, JETP Lett. **32**, 474 (1980); Phys. Lett. **B116**, 459 (1982).
- [25] A. Capella and J. Tran Thanh Van, Phys. Lett. **B114**, 450 (1982).
- [26] B. Andersson *et al.*, Phys. Rep. **97**, 31 (1983).
- [27] E. Gotsman and S. Nussinov, Phys. Rev. **D22**, 624 (1980).
- [28] R. Baier, Yu.L. Dokshitzer, A.H. Mueller, and D. Schiff, JHEP **0109**, 033 (2001).
- [29] B.G. Zakharov, JETP Lett. **88**, 781 (2008) [arXiv:0811.0445 [hep-ph]].
- [30] A. Gasher, H. Neuberger, and S. Nussinov, Phys. Rev. **D20**, 179 (1979).
- [31] A. Beraudo, J.G. Milhano, and U.A. Wiedemann, arXiv:1107.1080 [hep-ph]; arXiv:1109.5025 [hep-ph].
- [32] P. Kroll and K. Passek-Kumericki, Phys. Rev. **D67**, 054017 (2003).
- [33] G. Veneziano, Nucl. Phys. **B117**, 519 (1976).
- [34] N. Cardoso, M. Cardoso, and P. Bicudo, arXiv:1108.1542[hep-lat].
- [35] A.B. Kaidalov and O.I. Piskunova, Z. Phys. **C30**, 145 (1986); G.H. Arakelian , A. Capella , A.B. Kaidalov, and Yu.M. Shabelski, Eur. Phys. J. **C26**, 81 (2002) [arXiv:hep-ph/0103337].
- [36] P. Maris, Few Body Syst. **32**, 41 (2002).
- [37] C.D. Roberts, Prog. Part. Nucl. Phys. **61**, 50 (2008), and references therein.
- [38] N.N. Nikolaev and B.G. Zakharov, Phys. Lett. **B327**, 149 (1994).

- [39] E.V. Shuryak, Rev. Mod. Phys. **65**, 1 (1993).
- [40] R. Baier, Y.L. Dokshitzer, A.H. Mueller, S. Peigne, and D. Schiff, Nucl. Phys. B**484**, 265 (1997).
- [41] B.G. Zakharov, JETP Lett. **63**, 952 (1996); *ibid* **65**, 615 (1997); **70**, 176 (1999).
- [42] B.G. Zakharov, Phys. Atom. Nucl. **61**, 838 (1998).
- [43] P. Lévai and U. Heinz, Phys. Rev. C**57**, 1879 (1998).
- [44] N.N. Nikolaev, W. Schafer, and B.G. Zakharov, Phys. Rev. D**72**, 114018 (2005) [arXiv:hep-ph/0508310].
- [45] N.N. Nikolaev, W. Schafer, B.G. Zakharov, and V.R. Zoller, Phys. Rev. D**72**, 034033 (2005) [arXiv:hep-ph/0504057].
- [46] N.N. Nikolaev and B.G. Zakharov, Z. Phys. C**49**, 607 (1991).
- [47] Yu.L. Dokshitzer, V.A. Khoze, and S.I. Troyan, Phys. Rev. D**53**, 89 (1996).
- [48] T. Sjostrand, L. Lonnblad, S. Mrenna, and P. Skands, arXiv:hep-ph/0308153.
- [49] B.G. Zakharov, JETP Lett. **80**, 617 (2004) [arXiv:hep-ph/0410321].
- [50] B.G. Zakharov, JETP Lett. **93**, 683 (2011) [arXiv:1105.2028 [hep-ph]].
- [51] J.D. Bjorken, Phys. Rev. D**27**, 140 (1983).
- [52] B. Müller and K. Rajagopal, Eur. Phys. J. C**43**, 15 (2005).
- [53] S. Albino, B.A. Kniehl, and G. Kramer, Nucl. Phys. B**803**, 42 (2008).
- [54] B.A. Kniehl, G. Kramer, and B. Potter, Nucl. Phys. B**582**, 514 (2000).
- [55] J. Adams, *et al.* [STAR Collaboration], Phys. Lett. B**637**, 161 (2006).